

Direct observation of ultrafast magnetization dynamics in Co/Ni bit patterned media by time-resolved scanning Kerr microscopy

Wei Zhang(张伟), Wei He(何为), Qin-Li Lv(吕琴丽), Jian-Wang Cai(蔡建旺), Xiang-Qun Zhang(张向群), and Zhao-Hua Cheng(成昭华)

Citation: Chin. Phys. B, 2025, 34 (**4**): 047501. DOI: 10.1088/1674-1056/adb67e
Journal homepage: http://cpb.iphy.ac.cn; http://iopscience.iop.org/cpb

What follows is a list of articles you may be interested in

Investigation of magnetization reversal and domain structures in perpendicular synthetic antiferromagnets by first-order reversal curves and magneto-optical Kerr effect

Xiang-Qian Wang(王向谦), Jia-Nan Li(李佳楠), Kai-Zhou He(何开宙),Ming-Ling Xie(谢明玲), and Xu-Peng Zhu(朱旭鹏)
Chin. Phys. B, 2023, 32 (**11**): 117502. DOI: 10.1088/1674-1056/acd8aa

Experimental observation of interlayer perpendicular standing spin wave mode with low damping in skyrmion-hosting $[Pt/Co/Ta]_{10}$ multilayer

Zhen-Dong Chen(陈振东), Mei-Yang Ma(马眉扬), Sen-Fu Zhang(张森富), Mang-Yuan Ma(马莽原), Zi-Zhao Pan(潘咨兆), Xi-Xiang Zhang(张西祥), Xue-Zhong Ruan(阮学忠), Yong-Bing Xu(徐永兵), and Fu-Sheng Ma(马付胜)
Chin. Phys. B, 2022, 31 (**11**): 117501. DOI: 10.1088/1674-1056/ac7bf9

Magnetic anisotropy manipulation and interfacial coupling in $Sm_3Fe_5O_{12}$ films and $CoFe/Sm_3Fe_5O_{12}$ heterostructures

Lei Shen(沈磊), Guanjie Wu(武冠杰), Tao Sun(孙韬), Zhi Meng(孟智), Chun Zhou(周春), Wenyi Liu(刘文怡), Kang Qiu(邱康), Zongwei Ma(马宗伟), Haoliang Huang(黄浩亮), Yalin Lu(陆亚林), Zongzhi Zhang(张宗芝), and Zhigao Sheng(盛志高)
Chin. Phys. B, 2021, 30 (**12**): 127502. DOI: 10.1088/1674-1056/ac0040

Antiferromagnetic spin dynamics in exchanged-coupled $Fe/GdFeO_3$ heterostructure

Na Li(李娜), Jin Tang(汤进), Lei Su(苏磊), Ya-Jiao Ke(柯亚娇), Wei Zhang(张伟), Zong-Kai Xie(谢宗凯), Rui Sun(孙瑞), Xiang-Qun Zhang(张向群), Wei He(何为), and Zhao-Hua Cheng(成昭华)
Chin. Phys. B, 2021, 30 (**11**): 117502. DOI: 10.1088/1674-1056/abf3b7

Manipulating magnetic anisotropy and ultrafast spin dynamics of magnetic nanostructures

Cheng Zhao-Hua (成昭华), He Wei (何为), Zhang Xiang-Qun (张向群), Sun Da-Li (孙达力), Du Hai-Feng (杜海峰), Wu Qiong (吴琼), Ye Jun (叶军), Fang Ya-Peng (房亚鹏), Liu Hao-Liang (刘郝亮)
Chin. Phys. B, 2015, 24 (**7**): 077505. DOI: 10.1088/1674-1056/24/7/077505

Direct observation of ultrafast magnetization dynamics in Co/Ni bit patterned media by time-resolved scanning Kerr microscopy

Wei Zhang(张伟)[1,2], Wei He(何为)[1,†], Qin-Li Lv(吕琴丽)[1,3], Jian-Wang Cai(蔡建旺)[1,4], Xiang-Qun Zhang(张向群)[1], and Zhao-Hua Cheng(成昭华)[1,4,5,‡]

[1] *State Key Laboratory of Magnetism and Beijing National Laboratory for Condensed Matter Physics, Institute of Physics, Chinese Academy of Sciences, Beijing* 100190, *China*
[2] *National Key Laboratory of Spintronics, Hangzhou International Innovation Institute, Beihang University, Hangzhou* 311115, *China*
[3] *Guobiao (Beijing) Testing & Certification Co., Ltd., China Grinm Group Co., Ltd., Beijing* 101407, *China*
[4] *School of Physical Sciences, University of Chinese Academy of Sciences, Beijing* 100049, *China*
[5] *Songshan Lake Materials Laboratory, Dongguan* 523808, *China*

(Received 6 December 2024; revised manuscript received 10 February 2025; accepted manuscript online 15 February 2025)

Bit patterned recording (BPR) has attracted much attention due to its promising potential in achieving high densities in magnetic storage devices. The materials with strong perpendicular magnetic anisotropy (PMA) are always preferred in designing the BPR. Here, the patterned Co/Ni multilayers showing d–d hybridization induced PMA was studied. In particular, we record the ultrafast spin dynamics by means of time-resolved scanning magneto-optical Kerr effect (TRMOKE) microscopy. We are able to acquire the "snapshot" magnetic maps of the sample surface because of both the femtosecond temporal and submicrometer spatial resolution in our TRMOKE microscopy. Furthermore, the spatially inhomogeneous ultrafast demagnetization was observed in experiment, and this has been evidenced by simulations.

Keywords: ultrafast spin dynamics, magneto-optical Kerr effect, micromagnetic simulations

PACS: 75.40.Gb, 75.78.Cd, 75.78.–n

DOI: 10.1088/1674-1056/adb67e **CSTR:** 32038.14.CPB.adb67e

1. Introduction

As compared with the continuous magnetic recording media, the magnetic island achieved by lithographically in bit patterned recording (BPR) is used to be a single bit. This makes BPR more applicable in contracting the spintronics devices with high density.[1] Meanwhile, the thermal stability is another key parameter in designing the magnetic data storage media.[2,3] As a result, the magnetic materials with high perpendicular magnetic anisotropy (PMA) is usually desirable. For instance, Yang *et al*. investigated the PMA in Fe/MgO[4] and Co/graphene[5] heterostructures structures via first-principles calculations. Even, they stated that the interfaces between ferromagnetic and heavy nonmagnetic transition metals such as Co/Pt, Co/Pd, and Co/Ni have been used to achieve high PMA. In these materials, the PMA comes from the strong hybridization between the 3d orbitals of transition metal and the 5d orbitals of the heavy metals. In fact, a lot of investigations[6–8] on the origin of the PMA as well as the Gilbert damping has been carried out, since they are critical for the modulation of both densities and power consumptions for magnetic recording media and magnetic random-access memories (MRAMS).

For the above-mentioned magnetic multilayers with PMA, the static magnetic properties and dynamics in nanosecond timescale have been extensively studied.[9,10] However, their ultrafast spin dynamics within picosecond timescale is largely unexplored. The fundamental and practical limit of the speed of magnetization reversal is a subject of vital importance for magnetic recording and information processing technologies as well as one of the most intriguing questions of modern magnetism. The conventional way to reverse the magnetization $\boldsymbol{M}$ is to apply a magnetic field $\boldsymbol{H}$ antiparallel to $\boldsymbol{M}$. In the case of static magnetic configurations, magnetic force microscopy provides highly detailed results against which numerical predictions can be tested. For dynamic phenomena, direct experimentation is also highly desirable, and may even stimulate the development of new phenomenological theory.

In this study, we investigate the ultrafast spin dynamics in Co/Ni patterned multilayers via both time-resolved scanning magneto-optical Kerr effect (TRMOKE) microscopy[11] and simulations, including atomistic and FDTD methods. We directly observed the "snapshot" magnetic maps of the sample surface thanks to the temporal and spatial resolution of TRMOKE equipment. Therefore, we are able to collect the first-hand insight into the magnetization development, observing nonuniform spatial profiles which would be invisible within other techniques such as a typical TRMOKE[12] without microscopy and Vector Network Analyzer ferromag-

†Corresponding author. E-mail: hewei@iphy.ac.cn
‡Corresponding author. E-mail: zhcheng@iphy.ac.cn

© 2025 Chinese Physical Society and IOP Publishing Ltd. All rights, including for text and data mining, AI training, and similar technologies, are reserved.

netic resonance (VNA-FMR).[13] Instead, they can only be used to extract the magnetization dynamics in time and frequency domain, respectively. This combination makes this technique a very powerful tool for fundamental as well as applied physics. For example, it has been used to direct visualize the nonuniform spin precession, magnetostatic waves, and spin waves.[14] More importantly, it could be quite sensitive for the local magnetization evolution as a function of time and space in the isolated area.

2. Results

A DC magnetron sputtering system is used to deposit thin films on water-cooled Si substrates. The thin film deposition process takes place at room temperature. The film structure is NiFeCr(30)/Cu(30)/[Co(1.5)/Ni(5)]$_5$/NiFeCr(30), and the thickness of each layer shown in parentheses is in units of Å. The background vacuum of the sputtering system is better than 4×10^{-5} Pa, and the Ar air pressure is maintained at 0.5 Pa. Each layer of film is deposited by the corresponding metal target, and the purity of the target material used is higher than 99.99%, and the thickness of each layer is controlled by sputtering time. In Fig. 1(a), the magnetic hysteresis loops of Co/Ni multilayer is shown. It was measured by applying a magnetic field perpendicular to the film. The easy magnetization axis was parallel to the film normal direction indicating the large PMA of the multilayer. The anisotropy field of this multilayer was estimated to be about $H_K = 2.3$ kOe (1 Oe = 79.5775 A·m^{-1}), and coercivity of $H_c = 150$ Oe and the normalized magnetization is about 0.91. The anisotropy field is estimated from an effective magnetic anisotropy, so that it includes both perpendicular magnetic anisotropy and shape anisotropy.

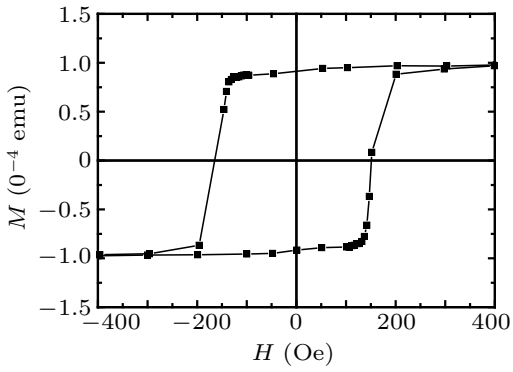


Fig. 1. Out of plane hysteresis loop obtained in [Co(1.5A)/Ni(5A)]$_5$ multilayer using VSM.

Figure 2(a) shows the TR-MOKE signals of the ultrafast demagnetization evolution after optical excitation.[15,16] For our TR-MOKE experimental setup, we used 780-nm laser as the pump with 55-fs pulse duration and the single pulse energy is around 100 nJ at 5.2-MHz repetition rate (For more details, please see our previous work[15]). A rapid decrease of magnetization takes place on the subpicosecond time scale, followed by a pronounced recovery. The time evolution of magnetization on picosecond timescales can be fitted according to Eq. (1) in terms of the three-temperature model (3TM)[15–17] which describes the energy distribution among electrons, phonons, and spins after laser excitation:

$$-\frac{\Delta M(t)}{M} = \left\{ \left[\frac{A_1}{(t/\tau_0+1)^{0.5}} - \frac{A_2\tau_E - A_1\tau_M}{\tau_E - \tau_M} e^{-t/\tau_M} - \frac{\tau_E(A_1 - A_2)}{\tau_E - \tau_M} e^{-t/\tau_E} \right] \Theta(t) \right\} \cdot G(t, \tau_G), \quad (1)$$

where $G(t, \tau_G)$ represents the convolution product with the Gaussian laser pulse profile and τ_G is the full width at half maximum of the laser pulses. $\Theta(t)$ is the Heaviside function. The constant A_1 represents the amplitude of demagnetization obtained after equilibrium between the electrons, spins, and phonons, while A_2 is proportional to the initial electron temperature raise. The two critical time parameters τ_M and τ_E are the ultrafast demagnetization time and magnetization recovery time, respectively. Here, the ultrafast demagnetization time extracted from Eq. (1) is 150 fs, which agrees well with previous reports in Co/Ni[16] or Co/Pt[18] ultrathin film with strong PMA.

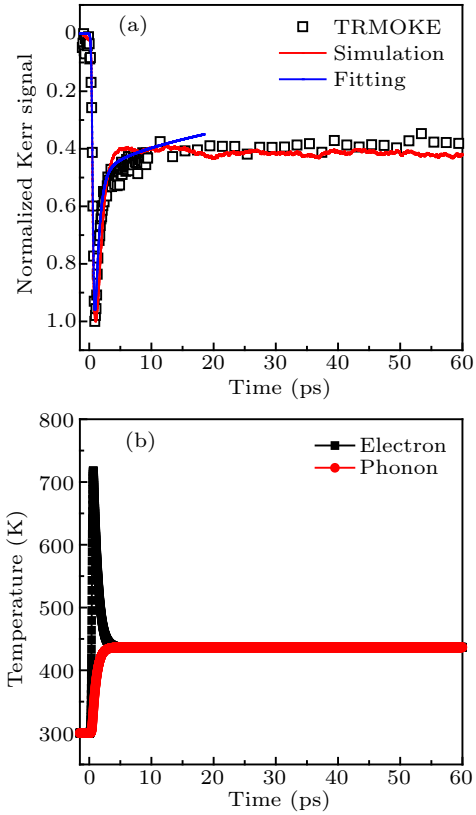


Fig. 2. (a) Ultrafast demagnetization curve obtained by TRMOKE measurement. The red line represents the numerical result using Vampire package and the blue one is the fitting curve from Eq. (1). (b) The evolution of electron and phonon temperature after the excitation of femtosecond laser pulse.

In order to understand the non-equilibrium process induced by femtosecond laser pulse in Co/Ni systems, the ultrafast demagnetization dynamics is simulated by means of

Vampire[19] software package. The dynamics of magnetization induced by laser pulse could be partially understood by the two-temperature model, which has been included in Vampire. Besides, for the magnetization system, the following Hamiltonian is used to describe all the energies included in the simulations:

$$H = -\sum_{i\neq j} J_{ij}\boldsymbol{S}_i\cdot\boldsymbol{S}_j - k_u\sum_i(\boldsymbol{S}_i\cdot\boldsymbol{e})^2 - \sum_i \mu_s\boldsymbol{S}_i\cdot\boldsymbol{H}_{\rm app}. \quad (2)$$

It is obvious that the first term is the Heisenberg exchange energy, where J_{ij} is the exchange interaction constant between the nearest neighboring two spins $\boldsymbol{S}_i$ and $\boldsymbol{S}_j$. Then, k_u represents the uniaxial anisotropy energy per atom, so the second term indicates the magnetocrystalline anisotropy for the whole system. And, the third one showing the Zeeman energy describes the interactions between the magnetic moments and the applied fields.

To obtain the laser induced magnetization dynamics, the typical Landau–Lifshitz–Gilbert equation has to be incorporated by Langevin dynamics, in which the thermal effect is taken into account by the term of $\boldsymbol{H}^i_{\rm eff}$:

$$\frac{\partial\boldsymbol{S}_i}{\partial t} = -\frac{\gamma}{(1+\lambda^2)}[\boldsymbol{S}_i\times\boldsymbol{H}^i_{\rm eff} + \lambda\boldsymbol{S}_i\times(\boldsymbol{S}_i\times\boldsymbol{H}^i_{\rm eff})], \quad (3)$$

where γ is the gyromagnetic ratio, λ is the microscopic damping parameter mainly coming from intrinsic contributions of spin-electron and spin–lattice interactions. $\boldsymbol{H}^i_{\rm eff}$ is the net magnetic field on each spin including an additional white noise term: $\boldsymbol{H}^i_{\rm th} = \Gamma(t)\sqrt{\frac{2\lambda k_{\rm B}T}{\gamma\mu_s\Delta t}}$, where $k_{\rm B}$ is the Boltzmann constant, T is the system temperature, Δt is the integration time step. And $\Gamma(t)$ is the Gaussian white noise term representing the thermal fluctuations on each atomic site. Therefore, the effective field in above LLG equation with Langevin Dynamics reads

$$\boldsymbol{H}^i_{\rm eff} = -\frac{1}{\mu_s}\frac{\partial H}{\partial\boldsymbol{S}_i} + \boldsymbol{H}^i_{\rm th}. \quad (4)$$

As mentioned above, the two-temperature model describing the interactions between electron and lattice system is always used to understand the laser-induced magnetization dynamics. In this model, the spin and electron system are closely coupled between each other. And finally, they equilibrated with the lattice leading to an equilibration temperature for the whole system. Such evolution of the system temperature is the driven force underlying the magnetization dynamics.

For the ferromagnetic structures constructed within Vampire software, the length and width of both Co and Ni layers are set as 30 nm with the periodic boundary conditions. The total height is set as 3.25 nm, where the ratio between Co and Ni is 1:5 in consistent with that in experiments. Meanwhile, we assume that the heat capacity of lattice $C_{\rm p}$ is independent of the lattice temperature and given by $C_{\rm p} = 8.5\times10^6$ J·m^{-3}·K^{-1}, while the electronic heat capacity $C_{\rm e}$ is proportional to the temperature $T_{\rm e}$ via $C_{\rm e} = \gamma T_{\rm e}$ with $\gamma = 3\times10^3$ J·m^{-3}·K^{-1}. The value of electron–lattice coupling parameter $G_{\rm e-p}$ is set as 1.5×10^{18} W·m^{-3}·K^{-1}. The values of all the parameters are consistent with those in literatures.[19,20]

In Fig. 2(a), the magnetization evolution as a function of time obtained in experiments is consistent with that within atomistic simulations. It indicates that the simulations combining the LLG equations with the two-temperature model is validated to understand the ultrafast demagnetization. Figure 2(b) shows the evolution of temperatures of electrons and phonons after the excitation by ultrashort laser pulse. The electronic system is driven to a high temperature firstly, and then pure energy transfer from the optically excited hot electrons to the lattice. As a result, both the electrons and phonons reach an equilibrium state after a typically 1 ps.

Figure 3 shows typical images of magnetic domains in Co/Ni multilayers at various time delays after excitation by laser pulses via our time-resolved scanning magneto-optical Kerr effect (TRMOKE) microscopy. The images were obtained for both types of domains with initial magnetization up and down. In the first few hundreds of femtoseconds, pump pulses bring the originally magnetized medium into a strongly non-equilibrium state with no measureable net magnetization. After sub-picosecond timescales, the magnetization recovers from the quenching state slowly. It is clearly that the demagnetization profile is non-uniform spatially. The amplitude of the response is largest in the middle, and then it propagates towards the edge.

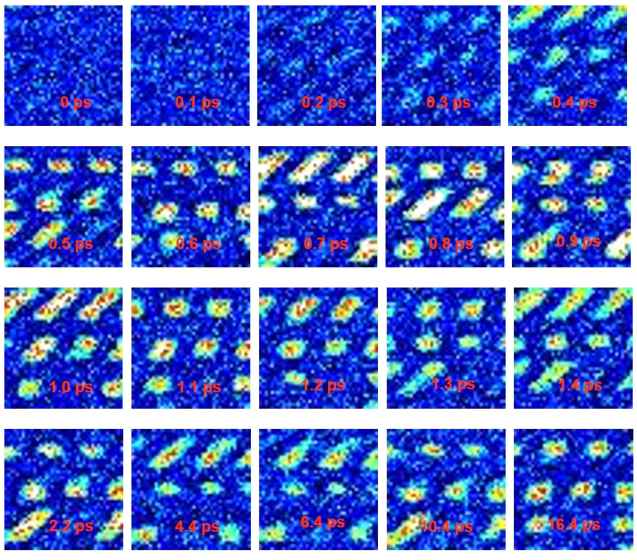


Fig. 3. Images of magnetic domains in Co/Ni multilayers at various time delays after excitation by laser pulses.

In order to understand this phenomenon, a commercial-grade simulator based on the finite-difference time-domain (FDTD) method[21] was used to calculate the laser absorption profiles within a two-dimensional plane. We considered a Gaussian distribution wave illumination at a wave-

length 800 nm, linearly p-polarized, impinging on the sample through a lens in order to agree with the experimental conditions. The light absorption per unit volume reads $P_{\text{abs}} = -0.5\omega|E|^2 \text{imag}(\varepsilon)$, we only need to know the electric field and the imaginary part of the permittivity which is easy to measure in an FDTD simulation.

As shown in Fig. 4(a), the absorption picture of Gaussian laser perpendicular to the thin film makes us clear that the middle region of the sample shows a stronger optical absorption and consequently the faster demagnetization rate in the middle region. This agrees well with the results obtained in our experiment. As the direction of incoming laser not aligning the normal axis, the optical absorption distribution shows asymmetric behaviors as illustrated in Fig. 4(b). Although the 10° incidence geometry was kept constant defined as the angle between the out-plane laser wave vector $\boldsymbol{k}$ and normal axis of the sample, the out-plane incoming laser wave vector $\boldsymbol{k}$ was varied. With the laser wave vector rotating counter clockwise, the intensity of light absorption in the edge around the projection of wave vector decreases, as is given in Fig. 5.

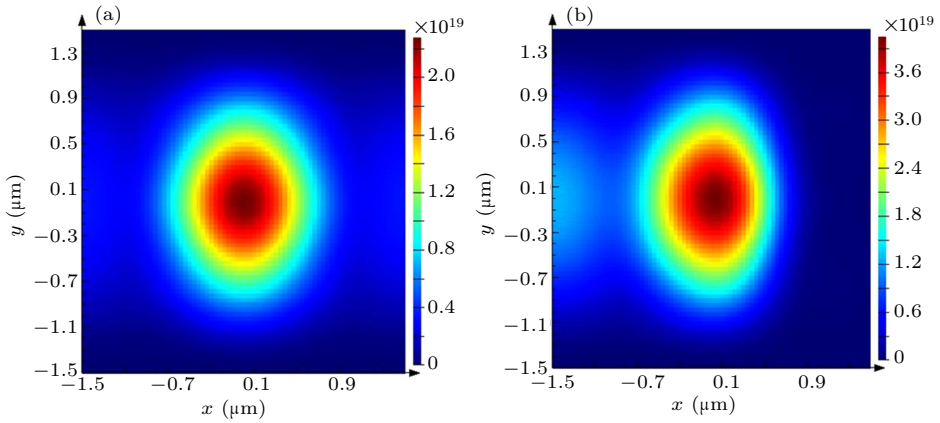


Fig. 4. FDTD-simulated light absorption inside thin films for perpendicular incoming laser (a) and 10° with respect to the normal axis (b).

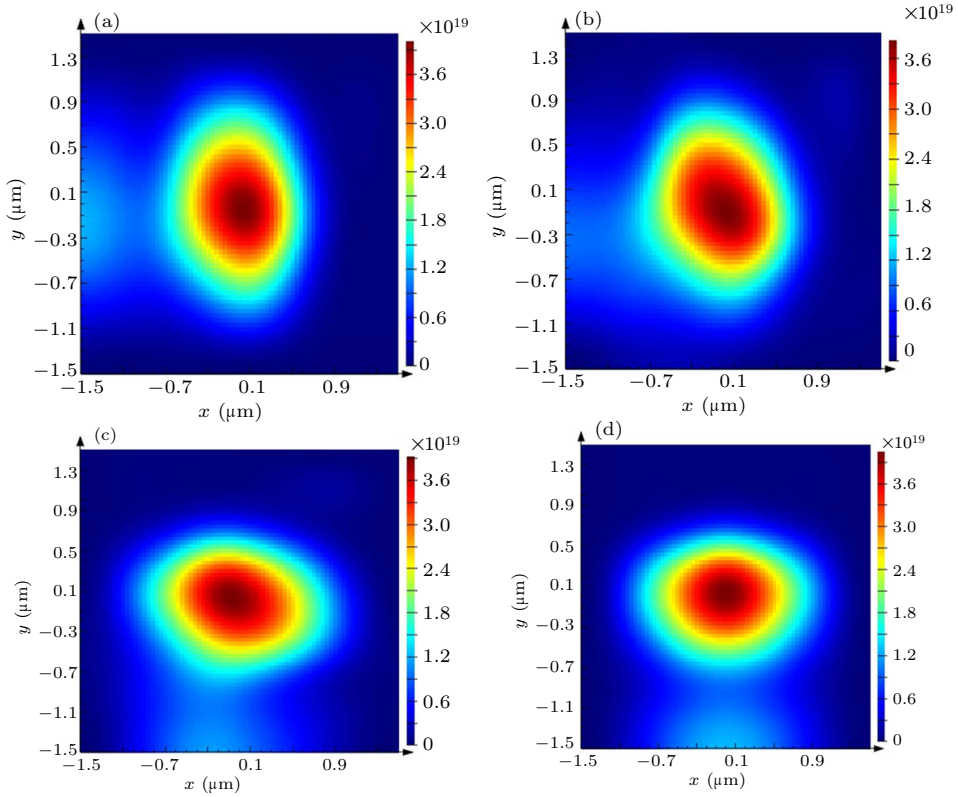


Fig. 5. FDTD-simulated light absorption inside thin films for various laser wave vector $\boldsymbol{k}$: (a) 10°, (b) 30°, (c) 50°, (d) 70°. The angle was defined between the projection of $\boldsymbol{k}$ in thin film and the plane composed of the incoming laser and normal axis.

3. Conclusion

In conclusion, we studied the magnetization dynamics taking place at picosecond timescale for ferromagnetic Co/Ni multilayers. By means of the time-resolved scanning Kerr microscopy technique as well as the atomistic simulations, the evolution of magnetization as a function of time was achieved from experiments and calculations, respectively. Moreover, we experimentally produced a group of dynamic MOKE im-

ages at different delay times. The non-uniform spatial demagnetization profile was explained based on an FDTD simulation, where the Gaussian shape laser absorption profiles was demonstrated. Such attempts with the time-resolved magnetic imaging techniques will provide deeper insights into interesting physics such as the microscopic mechanisms and interactions responsible for different types of magnetization dynamics.

Acknowledgements

Project supported by the National Key Research and Development Program of China (Grant No. 2022YFA1403302) and the National Natural Science Foundation of China (Grant Nos. 52031015, U22A20115, and 12104030), the Natural Science Foundation of Zhejiang Province, China (Grant No. LZ25A040007), and the Natural Science Foundation of Beijing (Grant No. 1252026).

References

[1] Richter H J, DobinI A Y, Heinonen O, Gao K Z, Veerdonk R J M V D, Lynch Q R T, Xue J, Weller P D, Asselin P, Erden M F and Brockie R M 2006 *IEEE Trans. Mag.* **42** 2255

[2] Daalderop G H O, Kelly P J and Broeder F J A D 1992 *Phys. Rev. Lett.* **68** 682

[3] Deng E Y, Deng E Y, Zhang Y, Klein J O, Ravelsona D, Chappert C and Zhao W S 2013 *IEEE Trants. Mag.* **49** 4982

[4] Yang H X, Chshiev M, Dieny B, Lee J H, Manchon A and Shi K H 2011 *Phys. Rev. B* **84** 054401

[5] Yang H X, Vu A D, Hallal A, Rougemaille N, Coraux J, Chen G, Schmid A K and Chshiev M 2016 *Nano Lett.* **16** 145

[6] Moore T A, Miron I M, Gaudin G, Serret G, Auffret S, Rodmacq B, Schuhl A, Pizzini Z, Vogel J and Bonfim M 2008 *Appl. Phys. Lett.* **93** 262504

[7] Yakushiji K, Saruya T, Kubota H, Fukushima A, Nagahama T, Yuasab S and Ando K 2010 *Appl. Phys. Lett.* **97** 232508

[8] Song H S, Lee K D, Sohn J W, Yang S H, Parkin S S P, You C Y and Shin S C 2013 *Appl. Phys. Lett.* **102** 102401

[9] Jiang S L, Chen X, Li X J, Yang K, Zhang J Y, Yang G, Liu Y W, Lu J H, Wang D W, Teng J and Yu G H 2015 *Appl. Phys. Lett.* **107** 112404

[10] Chen X, Wang K Y, Wu Z L, Jiang S L, Yang G, Liu Y, Teng J and Yu G H 2014 *Appl. Phys. Lett.* **104** 052413

[11] Li J, Lee M S, He W, Redeker B, Remhof A, Amaladass E, Hassel C and Eimüller T 2009 *Rev. Sci. Instrum.* **80** 073703

[12] Kampen M V, Jozsa C, Kohlhepp J T, LeClair P, Lagae L, Jonge W J M D and Koopmans B 2002 *Phys. Rev. Lett.* **88** 227201

[13] Kalarickal S S, Krivosik P, Wu M Z, Patton C E, Schneider M L, Kabos P, Silva T J and Nibarger J P 2006 *J. Appl. Phys.* **99** 093909

[14] Woltersdorf G, Buess M, Heinrich B and Back C H 2005 *Phys. Rev. Lett.* **95** 037401

[15] He W, Zhu T, Zhang X Q, Yang H T and Cheng Z H 2013 *Sci. Rep.* **3** 2883

[16] Zhang W, He W, Zhang X Q, Cheng Z H, Teng J and Fähnle M 2017 *Phys. Rev. B* **96** 220415

[17] Malinowski G, Longa F D, Rietjens J H H, Paluskar P V, Huijink R, Swagten H J M and Koopmans B 2008 *Nat. Phys.* **4** 855

[18] Kuiper K C, Roth T, Schellekens A J, Schmitt O, Koopmans B, Cinchetti M and Aeschlimann M 2014 *Appl. Phys. Lett.* **105** 202402

[19] Evans R F L, Fan W J, Chureemart P, Ostler T A, Ellis M O A and Chantrell R W 2014 *J. Phys.: Condens. Matter* **26** 103202

[20] Atxitia U 2020 *Modeling of ultrafast laser-induced magnetization dynamics within the Landau–Lifshitz-Bloch approach*, Ph. D. Dissertation (Instituto de Ciencia de Materiales de Madrid)

[21] Guyader L L, Savoini M, Moussaoui S E, Buzzi M, Tsukamoto A, Itoh A, Kirilyuk A, Rasing T, Kimel A V and Nolting F 2015 *Nat. Commun.* **6** 5839